

Oxidation State of Copper Ions in $(\text{La}_{0.7}\text{Sr}_{0.3})(\text{Mn}_{1-x}\text{Cu}_x)\text{O}_{3\pm\delta}$ Ceramics and Their Magnetic Properties

A. G. Belous*, O. I. V'yunov*, O. Z. Yanchevskii*,
A. I. Tovstolytkin**, and V. O. Golub**

* Vernadsky Institute of General and Inorganic Chemistry, National Academy of Sciences of Ukraine,
pr. Akademika Palladina 32/34, Kiev, 03680 Ukraine

** Institute of Magnetism, National Academy of Sciences of Ukraine,
bul'v. Vernadskogo 36b, Kiev, 03142 Ukraine
e-mail: belous@ionc.kar.net

Received March 4, 2005

Abstract—Bulk ceramic samples of $(\text{La}_{0.7}\text{Sr}_{0.3})(\text{Mn}_{1-x}\text{Cu}_x)\text{O}_{3\pm\delta}$ manganites are prepared by solid-state reactions. The unit-cell parameters and Mn–O bond distances in the manganites are determined using the Rietveld profile analysis method, and their magnetic properties are studied with the use of ferromagnetic resonance measurements. The results attest to the formation of solid solutions. Their lattice parameters follow Vegard's law. The way in which the saturation magnetization of the manganites varies with composition depends on x . For $x \leq 0.07$, the saturation magnetization is a weak function of composition; for $x > 0.07$, it drops rapidly with increasing x . These results can be understood under the assumption that the only oxidation state of copper in $(\text{La}_{0.7}\text{Sr}_{0.3})(\text{Mn}_{1-x}\text{Cu}_x)\text{O}_{3\pm\delta}$ is $2+$.

DOI: 10.1134/S0020168506030149

INTRODUCTION

There is wide research interest in $\text{La}_{1-x}\text{A}_x\text{MnO}_3$ (A = alkaline-earth metal) manganites with a distorted perovskite structure, motivated by the high sensitivity of their electrical properties to an applied magnetic field (colossal magnetoresistive response), which makes these materials potentially attractive for magnetoelectronic applications [1, 2]. In most instances, however, significant changes in their resistivity are only observed in large fields or at low temperatures, which limits their potential applications. Recent studies have shown that combined cation doping of $\text{La}_{1-x}\text{A}_x\text{MnO}_3$ manganites is an effective approach to enhancing their magnetoresistive response [3, 4].

The properties of such materials are commonly interpreted in terms of double exchange in the Mn^{3+} – O – Mn^{4+} system. It has been shown, however, in a number of studies that Jahn–Teller electron–phonon coupling and the tendency toward charge (orbital) ordering play an important role in the physics of manganites [3–5]. The relative contributions of these effects can be varied via substitutions on the lanthanum and manganese sites, which, therefore, may have a strong effect on the magnetic properties and magnetoresistive response of the manganites, leading in some instances to drastic changes in their behavior.

Considerable attention has been paid to the study of the lattice effects arising from partial substitutions of rare-earth metals with different ionic radii on the lanthanum site [6, 7]. Substitutions of both magnetic (e.g., Co, Ni, and Fe) and nonmagnetic (e.g., Ge, Al, and Cu) elements for manganese [8–11] were investigated in [8–11]. The results indicate that the magnetoresistance of the manganites in question can be enhanced substantially, in particular, by doping with copper [11].

The available information about the effect of copper doping on the electrical and magnetic properties of $\text{La}_{1-x}\text{A}_x\text{MnO}_3$ (A = Ca, Sr) is rather contradictory. On the one hand, copper doping was reported to notably enhance the magnetoresistance of these manganites, especially the one in small magnetic fields [12, 13]. Moreover, Yuan *et al.* [14] were able to considerably extend the temperature range in which the colossal magnetoresistance of the Ca-doped manganite was almost constant. On the other hand, the properties of Cu-doped manganites proved very sensitive to synthesis conditions. In particular, Ghosh *et al.* [15] and Troyanchuk *et al.* [16] reported that doping with 5% Cu reduced the resistivity of the $\text{La}_{0.7}\text{Sr}_{0.3}\text{MnO}_3$ solid solution by as much as 50% and slightly reduced (by ≈ 15 K) the temperature of its metal–insulator transition. An unusual influence of Cu doping on the electrical properties of $\text{La}_{0.7}\text{Sr}_{0.3}\text{MnO}_3$ was described by Sergeenkov *et al.* [17]. They found that doping with a

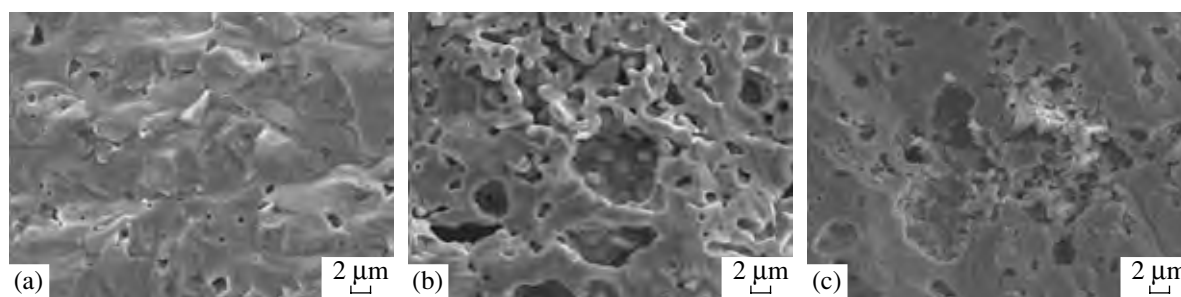


Fig. 1. Microstructures of $\text{La}_{0.7}\text{Sr}_{0.3}\text{Mn}_{1-x}\text{Cu}_x\text{O}_{3\pm\delta}$ ceramics with $x =$ (a) 0, (b) 0.05, and (c) 0.10.

small amount of Cu ($\approx 5\%$) caused the peak in resistivity as a function of temperature to split into two components. Anomalies in the electrical and magnetic properties of manganites lightly doped with copper and magnetic phase separation in such materials were revealed by various techniques, predominantly by resonance spectroscopies [12, 18–20]. Thus, there are considerable data that can be interpreted as evidence that copper substitution for manganese not only weakens the double exchange but also has a profound effect on the entire system of competing interactions characteristic of the manganites in question.

The properties of Cu-doped manganites are difficult to interpret or predict because the oxidation state of copper in these materials is still open to question. Typically, the copper ions in oxide compounds are in the oxidation state $2+$ [21], but Cu^+ and Cu^{3+} may also be present [22, 23]. Tikhonova [23] assumed that the observed reduction in unit-cell volume was due to Cu^{3+} substitution for Mn^{3+} . At the same time, Yuan *et al.* [12, 14, 18] and Ghosh *et al.* [15] interpreted their results under the assumption that all of the copper ions were in the oxidation state $2+$. Structural data for polycrystalline $\text{La}_{1-z}\text{Sr}_z\text{Mn}_{1-x}\text{Cu}_x\text{O}_3$ ($z = 0, 0.1, 0.3$; $x = 0-0.5$) materials led Tikhonova *et al.* [24] to conclude that both Cu^{2+} and Cu^{3+} ions were present. Similar conclusions were made in earlier studies [13, 25]. Thus, the reported data on the oxidation state of copper in the manganites under consideration are contradictory.

The objective of this work was to synthesize $(\text{La}_{0.7}\text{Sr}_{0.3})(\text{Mn}_{1-x}\text{Cu}_x)\text{O}_{3\pm\delta}$ solid solutions and to study their structural, magnetic, and resonance properties with the aim of determining the oxidation state of copper ions in these manganites.

EXPERIMENTAL

Polycrystalline $\text{La}_{0.7}\text{Sr}_{0.3}\text{Mn}_{1-x}\text{Cu}_x\text{O}_{3\pm\delta}$ (LSMC) ($x = 0-0.15$) samples for this investigation were prepared by solid-state reactions, using extrapure-grade La_2O_3 and Mn_2O_3 and reagent-grade SrCO_3 and CuO as raw materials. The starting mixtures were homogenized by milling with bidistilled water. After drying at 370–390 K, the mixtures were screened through a 65 mesh

nylon-6 sieve and then fired at 1270 K for 4 h. The resultant powder was pressed into disks 12 mm in diameter and 3 mm in thickness, which were then sintered at $T_{\text{sint}} = 1540-1600$ K for 2 h.

X-ray diffraction (XRD) measurements were performed on a DRON 4-07 powder diffractometer (CoK_α radiation, 40 kV, 20 mA, $2\theta = 10^\circ-150^\circ$, step-scan mode with a step size $\Delta(2\theta) = 0.02^\circ$ and a counting time of 10 s per data point). Structural parameters were refined by the Rietveld profile analysis method, using the FullProf program. As external standards, we used SiO_2 (2θ calibration) and Al_2O_3 (NIST SRM1976 intensity standard). The Mn^{3+} and Mn^{4+} contents of the samples were determined by titrating iodine with a sodium thiosulfate solution. Iodine in a potassium iodide solution was replaced by chlorine released upon dissolution of a manganite sample in hydrochloric acid [26]. In analyzing the structural aspects of copper substitution for manganese, calculations were performed as proposed by Ullmann and Trofimenko [27], using Shannon's system of ionic radii [28].

Magnetization was measured with a Quantum Design MPMS-5S SQUID magnetometer. Ferromagnetic resonance (FMR) studies were performed on a RADIOPAN spectrometer (9.2 GHz), using samples $1 \times 1 \times 5$ mm in dimensions. The applied magnetic field was parallel to the long axis of the sample.

RESULTS AND DISCUSSION

Figure 1 shows micrographs of $\text{La}_{0.7}\text{Sr}_{0.3}\text{Mn}_{1-x}\text{Cu}_x\text{O}_{3\pm\delta}$ ceramic samples sintered in air at 1300°C . The three samples are seen to consist of fine grains about $2 \mu\text{m}$ in size. With increasing x , the porosity of the ceramics increases slightly.

The $\text{La}_{0.7}\text{Sr}_{0.3}\text{Mn}_{1-x}\text{Cu}_x\text{O}_{3\pm\delta}$ ceramics prepared by sintering in air at 1300°C had a distorted perovskite structure (sp. gr. $R\bar{3}c$) with La(Sr) in position $6a$ ($0\ 0\ 1/4$), Mn(Cu) in $6b$ ($0\ 0\ 0$), and O in $18e$ ($x\ 0\ 1/4$). The lattice parameters of the samples were refined by the Rietveld profile analysis method (Fig. 2). Copper substitution

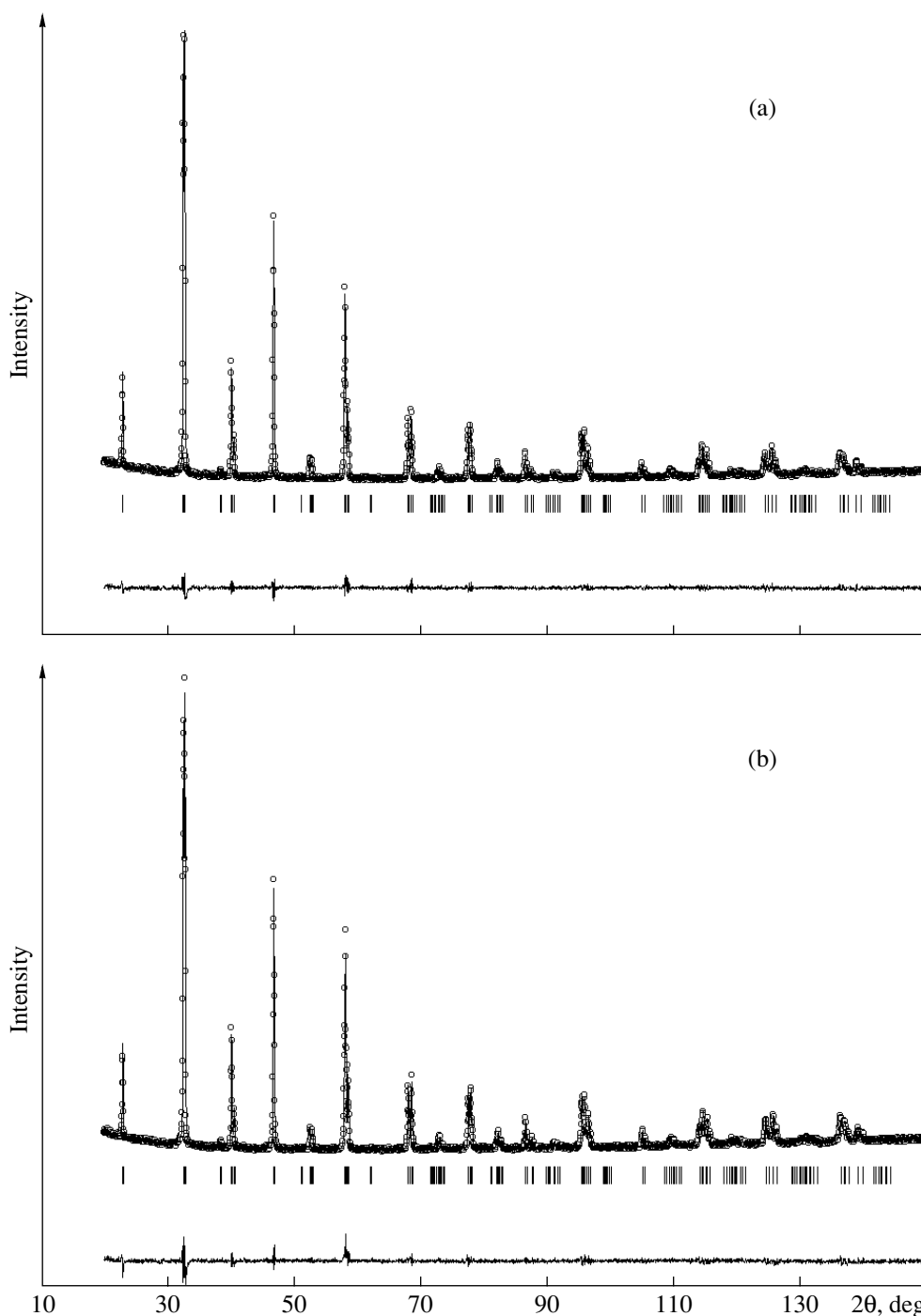


Fig. 2. Raw XRD data (points), calculated profile (continuous line), and difference plot (lower continuous line) for (a) $\text{La}_{0.7}\text{Sr}_{0.3}\text{Mn}_{0.95}\text{Cu}_{0.05}\text{O}_3$ and (b) $\text{La}_{0.7}\text{Sr}_{0.3}\text{Mn}_{0.90}\text{Cu}_{0.10}\text{O}_3$ at room temperature; the vertical tick marks show the positions of allowed reflections.

for manganese was found to reduce the unit-cell volume and the positional parameter of oxygen (Table 1).

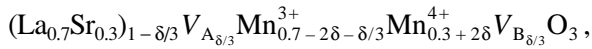
To determine the oxidation state of copper, the Rietveld refinement results were compared with different models for charge compensation in Cu-doped manganites. In calculations, we took into account that manganites may contain Mn^{3+} and Mn^{4+} . Mn^{2+} may only

appear if the material contains an appreciable concentration of lanthanum vacancies [29], whereas oxygen vacancies do not lead to the formation of Mn^{2+} [30]. According to chemical analysis data, the oxygen nonstoichiometry in $\text{La}_{0.7}\text{Sr}_{0.3}\text{Mn}_{1-x}\text{Cu}_x\text{O}_{3\pm\delta}$ with $x = 0$ was rather small, $\delta = +0.035$, which allowed Mn^{2+} formation to be left out of consideration. In connection with

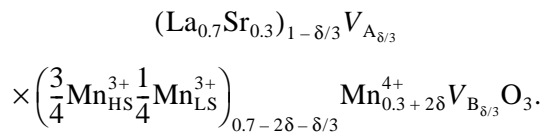
Table 1. Crystal data for La_{0.7}Sr_{0.3}Mn_{1-x}Cu_xO_{3±δ} manganites

<i>x</i>	0.000	0.01	0.025	0.04	0.050	0.075	0.100	0.125	0.150
<i>a</i> , Å	5.5061(2)	5.5070(1)	5.5054(2)	5.5057(2)	5.5047(5)	5.5043(2)	5.5017(3)	5.5017(2)	5.5000(3)
<i>c</i> , Å	13.3616(3)	13.3592(2)	13.3560(3)	13.3556(2)	13.3481(7)	13.3470(3)	13.3396(4)	13.3371(4)	13.3321(4)
<i>V</i> , Å ³	350.81(2)	350.86(1)	350.58(2)	350.61(2)	350.28(5)	350.20(2)	349.67(3)	349.61(2)	349.26(3)
<i>x</i> _O	0.464(3)	0.464(2)	0.464(2)	0.461(2)	0.460(3)	0.457(2)	0.456(2)	0.456(2)	0.456(2)
<i>R</i> _B , %	5.91	5.34	6.81	4.09	8.89	6.12	6.48	6.73	6.68
<i>R</i> _f , %	7.17	6.01	8.72	5.73	8.92	7.73	7.40	8.34	7.92
ρ _{meas} , g/cm ³	5.12	5.10	5.06	5.00	4.98	4.94	4.9	4.84	4.76

this, we assumed in calculations that manganese is in the oxidation states 3+ and 4+, whereas copper may be present in all of the possible oxidation states (1+, 2+, and 3+). The positive value of δ in La_{0.7}Sr_{0.3}MnO_{3+δ} is attributable to the presence of cation vacancies. As shown by Ullmann and Trofimenko [27], the general formula of the solid solution can then be represented in the form



where *V*_A and *V*_B are A-site and B-site vacancies in the ABO₃ perovskite. Based on temperature-dependent thermopower data for strontium-doped manganites, Hiroyuki Kamata *et al.* [31] showed that the Mn³⁺ ions in the La_{0.8}Sr_{0.2}MnO₃ solid solution are present in both high-spin (HS) and low-spin (LS) states, with Mn³⁺_{HS} : Mn³⁺_{LS} ≈ 3 : 1. The coexistence of Mn³⁺_{HS} and Mn³⁺_{LS} was confirmed both experimentally [32] and theoretically [33]. Therefore, the general formula of the strontium-doped manganites studied here can be represented as



Analyzing structural data for many A_{1-a}A'_aB_{1-b}B'_bO_{3±δ} perovskite oxides, Ullmann and Trofimenko [27] derived a relation between the free volume per unit cell, *V*_f, and the tolerance factor, *t*:

$$V_f = (1.20 \pm 0.09) - (0.95 \pm 0.09)t. \quad (1)$$

Here,

$$t = \frac{\langle \text{A-O} \rangle}{\sqrt{2} \langle \text{B-O} \rangle}, \quad (2)$$

$$V_f = \frac{V_{\text{meas}} - V_{\text{occ}}}{V_{\text{meas}}}, \quad (3)$$

where ⟨A–O⟩ and ⟨B–O⟩ are the mean cation–oxygen bond distances for the A and B cations, respectively; *V*_{meas} is the experimentally determined unit-cell volume; and *V*_{occ} is the occupied volume per unit cell, evaluated as the sum of the ion and vacancy volumes determined using the ionic radii of A, B, and O. In calculations, we assumed the presence of La³⁺ (*r* = 1.36 Å) and Sr²⁺ (1.44 Å) in the A sublattice; Mn³⁺_{HS} (0.645 Å), Mn³⁺_{LS} (0.72 Å), Mn⁴⁺ (0.53 Å), Cu⁺ (0.77 Å), Cu²⁺ (0.73 Å), and Cu³⁺ (0.54 Å) in the B sublattice; and O²⁻ (1.36 Å) in the anion sublattice. The radii of cation vacancies for δ > 0 (oxygen hyperstoichiometry) were evaluated by the formulas

$$r_{V_A} \approx r_A \sqrt[3]{V_f}, \quad r_{V_B} \approx r_B \sqrt[3]{V_f}. \quad (4)$$

From Eqs. (1) and (3), we obtain

$$V_{\text{meas}} = V_{\text{occ}} / (0.95t - 0.2), \quad (5)$$

$$\Delta V_{\text{meas}} = V_{\text{occ}} (0.09t - 0.09) / (0.95t - 0.2)^2.$$

Equations (2), (4), and (5) were used to calculate the unit-cell volumes and bond distances in La_{0.7}Sr_{0.3}Mn_{1-x}Cu_xO_{3±δ} solid solutions using different models for charge compensation in the Cu-containing manganese sublattice. Figure 3 shows the experi-

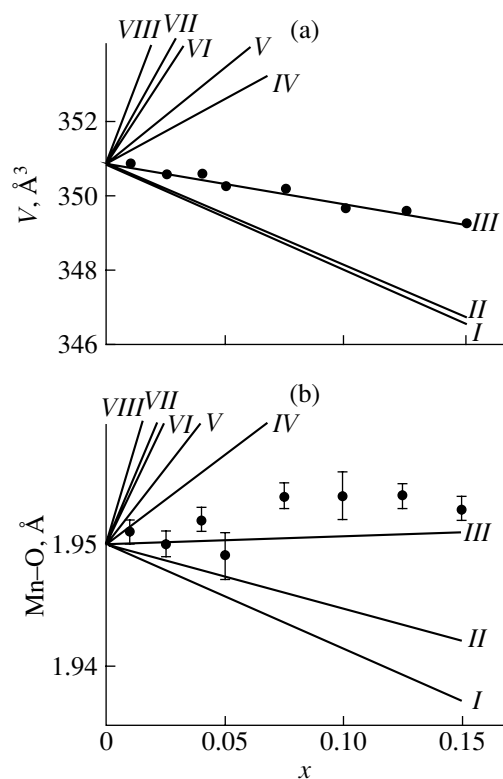


Fig. 3. (a) Unit-cell volume and (b) Mn–O bond distance as functions of copper content for $\text{La}_{0.7}\text{Sr}_{0.3}\text{Mn}_{1-x}\text{Cu}_x\text{O}_{3\pm\delta}$: experimental data (points) in comparison with calculation results in different models for charge compensation in the manganese sublattice (numbers at the curves identify models as referenced in Table 2).

mentally determined unit-cell volumes and Mn–O bond distances as functions of Cu content for $\text{La}_{0.7}\text{Sr}_{0.3}\text{Mn}_{1-x}\text{Cu}_x\text{O}_{3\pm\delta}$ in comparison with those cal-

culated in different models for charge compensation in Cu-doped manganites (Table 2). As seen in Fig. 3, the experimental data agree best with the charge compensation mechanism $2\text{Mn}^{3+} \rightarrow \text{Mn}^{4+} + \text{Cu}^{2+}$.

To assess the effect of the oxidation state of copper on the physical properties of the manganites, we measured their saturation magnetization M_s and FMR spectra at different copper concentrations. Figure 4 shows the 10-K M – H hysteresis loops of $\text{La}_{0.7}\text{Sr}_{0.3}\text{Mn}_{1-x}\text{Cu}_x\text{O}_{3\pm\delta}$ samples. In all of the samples except $\text{La}_{0.7}\text{Sr}_{0.3}\text{Mn}_{0.85}\text{Cu}_{0.15}\text{O}_3$, magnetization saturates for $H \geq 400$ kA/m.

Figure 5a shows the composition dependence of 10-K saturation magnetization M_s measured in a magnetic field of 4000 kA/m. The $M_s(x)$ behavior is seen to change sharply at $x = 0.07$: for $x \leq 0.07$, the saturation magnetization gradually decreases with increasing x ; for $x > 0.07$, it decreases far more steeply, remaining an almost linear function of x . Also shown in Fig. 5a is the $M_s(x)$ line calculated in model III. In calculations, the magnetic moments were taken to be $4\mu_B$ for $\text{Mn}_{\text{HS}}^{3+}$ ($S = 2$), $2\mu_B$ for $\text{Mn}_{\text{LS}}^{3+}$ ($S = 1$), and $3\mu_B$ for $\text{Mn}_{\text{HS}}^{3+}$ ($S = 3/2$) [3]. As seen, the experimental data and calculation results agree reasonably well for $x \leq 0.07$ but differ markedly for $x > 0.07$.

To rationalize these findings, we analyzed the fraction of Mn^{4+} (with respect to total manganese) as a function of copper content. The fraction of Mn^{4+} was evaluated from chemical analysis data for $x = 0$ [26] and using the model scheme $2\text{Mn}^{3+} \rightarrow \text{Mn}^{4+} + \text{Cu}^{2+}$ for $x > 0$ (Fig. 5b). Sr-doped manganites are known to contain a ferromagnetic phase if the fraction of Mn^{4+} lies in the range 0.18 to 0.50 [34, 35] (dashed region in Fig. 5b). Beyond this range, there is a tendency toward

Table 2. Models for charge compensation in $\text{La}_{0.7}\text{Sr}_{0.3}\text{Mn}_{1-x}\text{Cu}_x\text{O}_{3\pm\delta}$

Model	Cation vacancies (oxygen hyperstoichiometry: $x < x_c$, $\delta > 0$)	Critical Cu content* for $\delta_0 = +0.035$ ($x_c = \delta = 0$)	Anion vacancies (cation hyperstoichiometry: $x > x_c$, $\delta < 0$)
I		$\text{Mn}^{3+} \rightarrow \text{Cu}^{3+**}$	
II		$3\text{Mn}^{3+} \rightarrow 2\text{Mn}^{4+} + \text{Cu}^+$	
III		$2\text{Mn}^{3+} \rightarrow \text{Mn}^{4+} + \text{Cu}^{2+}$	
IV	$2\text{Mn}^{4+} \rightarrow 2\text{Cu}^{3+} - 1/3(V_A + V_B)$	0.070	$2\text{Mn}^{4+} \rightarrow 2\text{Cu}^{3+} + V_{\text{O}}^{\bullet\bullet}$
V	$2\text{Mn}^{3+} \rightarrow 2\text{Cu}^{2+} - 1/3(V_A + V_B)$	0.070	$2\text{Mn}^{3+} \rightarrow 2\text{Cu}^{2+} + V_{\text{O}}^{\bullet\bullet}$
VI	$\text{Mn}^{3+} \rightarrow \text{Cu}^+ - 1/3(V_A + V_B)$	0.035	$\text{Mn}^{3+} \rightarrow \text{Cu}^+ + V_{\text{O}}^{\bullet\bullet}$
VII	$\text{Mn}^{4+} \rightarrow \text{Cu}^{2+} - 1/3(V_A + V_B)$	0.035	$\text{Mn}^{4+} \rightarrow \text{Cu}^{2+} + V_{\text{O}}^{\bullet\bullet}$
VIII	$2\text{Mn}^{4+} \rightarrow 2\text{Cu}^+ - (V_A + V_B)$	0.024	$2\text{Mn}^{4+} \rightarrow 2\text{Cu}^+ + 3V_{\text{O}}^{\bullet\bullet}$

* With increasing copper content, δ remains unchanged in models I–III and decreases, down to zero at x_c , in models IV–VIII.

** In calculations, we assumed a constant $\text{Mn}_{\text{HS}}^{3+} : \text{Mn}_{\text{LS}}^{3+}$ ratio in the Cu-doped manganites.

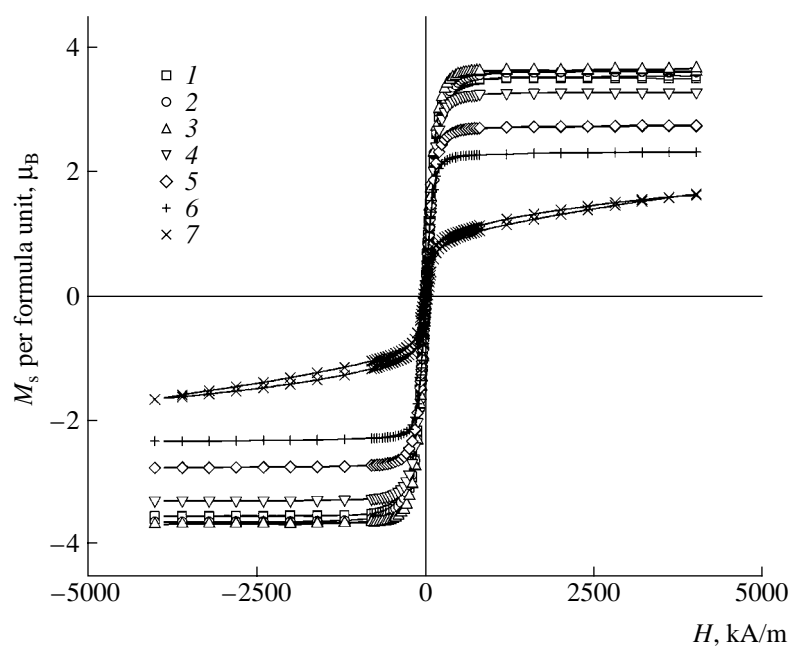


Fig. 4. M - H hysteresis loops of $\text{La}_{0.7}\text{Sr}_{0.3}\text{Mn}_{1-x}\text{Cu}_x\text{O}_{3\pm\delta}$ samples with $x = (1) 0$, (2) 0.025, (3) 0.050, (4) 0.075, (5) 0.100, (6) 0.125, and (7) 0.150; $T = 10$ K.

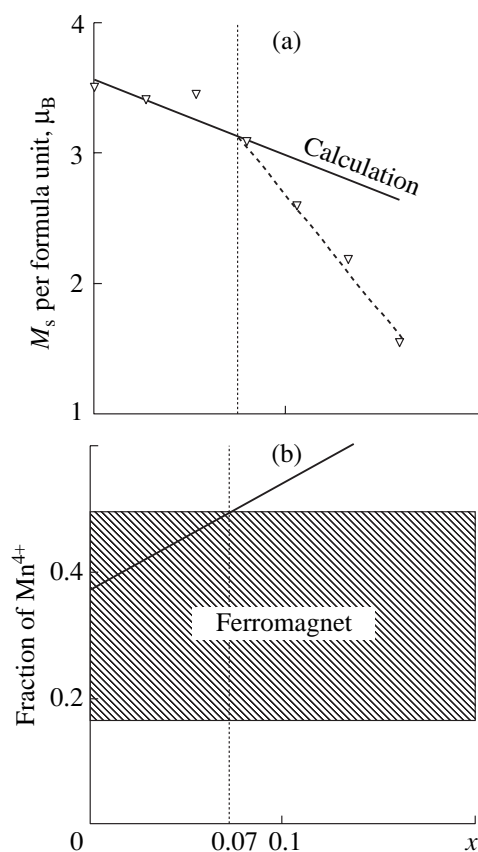


Fig. 5. (a) Composition dependences of the measured and calculated saturation magnetization for $\text{La}_{0.7}\text{Sr}_{0.3}\text{Mn}_{1-x}\text{Cu}_x\text{O}_{3\pm\delta}$ samples at 10 K in a magnetic field of 4000 kA/m. (b) Fraction of Mn^{4+} in $\text{La}_{0.7}\text{Sr}_{0.3}\text{Mn}_{1-x}\text{Cu}_x\text{O}_{3\pm\delta}$.

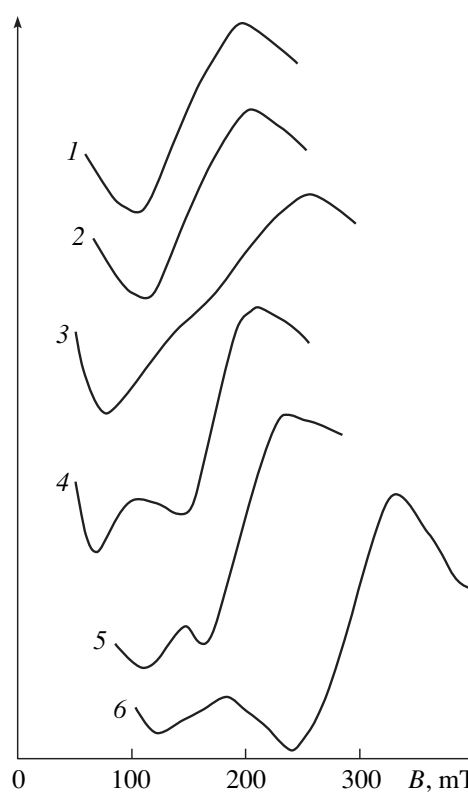


Fig. 6. 77-K FMR spectra of $\text{La}_{0.7}\text{Sr}_{0.3}\text{Mn}_{1-x}\text{Cu}_x\text{O}_{3\pm\delta}$ samples with $x = (1) 0$, (2) 0.025, (3) 0.050, (4) 0.075, (5) 0.100, and (6) 0.50.

antiferromagnetic ordering, which results in antiferromagnetism or more complex magnetic ordering [34, 35]. It follows from Fig. 5b that, for $x > 0.07$, the magnetic phase is likely to decompose into two phases, one of which has a low magnetization with no saturation in a magnetic field of 4000 kA/m. To verify this hypothesis, we measured the FMR spectra of $\text{La}_{0.7}\text{Sr}_{0.3}\text{Mn}_{1-x}\text{Cu}_x\text{O}_{3\pm\delta}$ samples.

Figure 6 illustrates the effect of copper content on the FMR spectrum. At $x = 0$ and 0.025, the spectra show a single signal whose parameters correspond to ferromagnetic ordering of the manganites and agree well with earlier data for $\text{La}_{0.7}\text{Sr}_{0.3}\text{MnO}_3$ (resonance field $B_r \approx 220$ mT, linewidth $w \approx 105$ mT) [36, 37]. At $x = 0.050$, the signal is slightly broadened, attesting to magnetic inhomogeneity. The salient feature of the magnetic resonance in the samples with $x > 0.070$ is the presence of two, well-resolved signals, corresponding to two distinct magnetic phases. These findings correlate well with the assumption that the samples with $x \leq 0.07$ consist of a homogeneous ferromagnetic phase, whereas those with $x > 0.07$ consist of two magnetic phases. Moreover, they lend support to the charge compensation mechanism $2\text{Mn}^{3+} \rightarrow \text{Mn}^{4+} + \text{Cu}^{2+}$ in $\text{La}_{0.7}\text{Sr}_{0.3}\text{Mn}_{1-x}\text{Cu}_x\text{O}_{3\pm\delta}$, according to which the copper in the manganites is in the oxidation state 2+.

CONCLUSIONS

The unit-cell volume, Mn–O bond distances, saturation magnetization, and FMR spectra of $\text{La}_{0.7}\text{Sr}_{0.3}\text{Mn}_{1-x}\text{Cu}_x\text{O}_{3\pm\delta}$ manganites indicate that the mechanism of charge compensation in the manganese sublattice containing copper ions can be represented by the scheme $2\text{Mn}^{3+} \rightarrow \text{Mn}^{4+} + \text{Cu}^{2+}$, according to which the copper is in the oxidation state 2+.

REFERENCES

1. Von Helmolt, R., Wecker, J., Samwer, K., *et al.*, Intrinsic Giant Magnetoresistance of Mixed Valence La–A–Mn Oxide (A = Ca, Sr, Ba), *J. Appl. Phys.*, 1994, vol. 76, no. 10, pp. 6925–6928.
2. Jin, S.S., Tiefel, T.H., McCormack, M., *et al.*, Thousand-fold Change in Resistivity in Magnetoresistive La–Ca–Mn–O Films, *Science*, 1994, vol. 264, no. 5157, pp. 413–415.
3. Haghiri-Gosnet, A.-M. and Renard, J.-P., CMR Manganites: Physics, Thin Films, and Devices, *J. Phys. D: Appl. Phys.*, 2003, vol. 36, pp. R127–R150.
4. Hwang, H.Y., Cheong, S.-W., Radaelli, P.G., *et al.*, Lattice Effects on the Magnetoresistance in Doped LaMnO_3 , *Phys. Rev. Lett.*, 1995, vol. 75, no. 5, pp. 914–917.
5. Gor'kov, L.P. and Kresin, V.Z., Manganites at Low Temperatures and Light Doping: Band Approach and Percolation, *Pis'ma Zh. Eksp. Teor. Fiz.*, 1998, vol. 67, no. 11, pp. 934–939.
6. Radaelli, P.G., Iannone, G., Marezio, M., *et al.*, Structural Effects on the Magnetic and Transport Properties of Perovskite $\text{A}_{1-x}\text{A}'_x\text{MnO}_3$ ($x = 0.25, 0.30$), *Phys. Rev. B: Condens. Matter*, 1997, vol. 56, p. 8265.
7. Pierre, J., Nossou, A., Vassiliev, V., and Ustinov, V., A Magnetic Pair-Breaking Effects in Rare Earth-Doped Manganites, *Phys. Lett. A*, 1998, vol. 250, pp. 435–438.
8. Rubinstein, M., Gillespie, D.J., Snyder, E.J., and Tritt, M.T., Effects of Gd, Co, and Ni Doping in $\text{La}_{2/3}\text{Ca}_{1/3}\text{MnO}_3$: Resistivity, Thermopower, and Paramagnetic Resonance, *Phys. Rev. B: Condens. Matter*, 1997, vol. 56, no. 9, pp. 5412–5423.
9. Sun, J.R., Rao, G.H., Shen, B.G., and Wong, H.K., Doping Effects Arising from Fe and Ge for Mn in $\text{La}_{0.7}\text{Ca}_{0.3}\text{MnO}_3$, *Appl. Phys. Lett.*, 1998, vol. 73, p. 2998.
10. Turilli, G. and Licci, F., Relationship between Spin Order and Transport and Magnetotransport Properties in $\text{La}_{0.67}\text{Ca}_{0.33}\text{Mn}_{1-x}\text{Al}_x\text{O}_3$ Compounds, *Phys. Rev. B: Condens. Matter*, 1996, vol. 54, no. 18, pp. 13052–13057.
11. Hebert, S., Maignan, A., Martin, C., and Raveau, B., Important Role of Impurity e_g Levels on the Ground State of Mn-Site Doped Manganites, *Solid State Commun.*, 2002, vol. 121, pp. 229–234.
12. Yuan, S.L., Yang, Y.P., Xia, Z.C., *et al.*, Unusual Hysteresis and Giant Low-Field Magnetoresistance in Polycrystalline Sample with Nominal Composition of $\text{La}_{2/3}\text{Ca}_{1/3}\text{Mn}_{0.955}\text{Cu}_{0.045}\text{O}_3$, *Phys. Rev. B: Condens. Matter*, 2002, vol. 66, pp. 172402-1–172402-4.
13. Nguyen, C., Niem, P.Q., Nhat, H.N., *et al.*, Influence of Cu Substitution for Mn on the Structure, Magnetic, Magnetocaloric, and Magnetoresistance Properties of $\text{La}_{0.7}\text{Sr}_{0.3}\text{MnO}_3$ Perovskites, *Physica B (Amsterdam)*, 2003, vol. 327, pp. 214–217.
14. Yuan, S.L., Tang, J., Xia, Z.C., *et al.*, Low-Field Colossal Constant Magnetoresistance for Wide Temperature Ranges in the Sol–Gel Prepared $\text{La}_{2/3}\text{Ca}_{1/3}\text{Mn}_{0.96}\text{Cu}_{0.04}\text{O}_3$, *Solid. State Commun.*, 2003, vol. 127, pp. 743–747.
15. Ghosh, K., Ogale, S.B., Ramesh, R., *et al.*, Transition-Element Doping Effects in $\text{La}_{0.7}\text{Ca}_{0.3}\text{MnO}_3$, *Phys. Rev. B: Condens. Matter*, 1999, vol. 59, no. 1, pp. 533–537.
16. Troyanchuk, O., Khalyavin, D.D., Shapovalova, E.F., *et al.*, *Proc. 8th Eur. Magnetic Materials and Application Conf.*, Kyiv, 2000, p. 34.
17. Sergeenkov, S., Ausloos, M., Vougrine, H., *et al.*, Anomalous Temperature Behavior of Resistivity in Lightly Doped Manganites around a Metal–Insulator Phase Transition, *Pis'ma Zh. Eksp. Teor. Fiz.*, 1999, vol. 70, no. 7, pp. 473–478.
18. Yuan, C.L., Zhu, Y., and Ong, P.P., The Effects of Cu Doping on the Magnetoresistive Behavior of Perovskites $\text{La}_{0.7}\text{Ca}_{0.3}\text{MnO}_3$, *Solid. State Commun.*, 2001, vol. 120, pp. 495–499.
19. Tovstolytkin, A.I., Pogorilyi, A.N., Shypil, E.V., and Podyalovski, D.I., An Abnormal Effect of Low Level Cu Doping on the Magnetism and Conductivity of $\text{La}_{0.7}\text{Ca}_{0.3}\text{MnO}_{3-\delta}$, *Phys. Met. Metallogr.*, 2001, vol. 91, suppl. 1, pp. S214–S218.

20. Reis, M.S., Freitas, J.C.C., Orlando, M.T.D., *et al.*, Electric and Magnetic Properties of Cu-Doped La–Sr Manganites, *J. Magn. Magn. Mater.*, 2002, vol. 668, pp. 242–245.
21. Haupt, L., Helmolt, R., Sondermann, U., *et al.*, Metal–Semiconductor Transition in the Double Exchange System $\text{La}_{0.8}\text{Sr}_{0.2}\text{Mn}_{1-x}\text{Cu}_x\text{O}_3$, *Phys. Lett. A*, 1992, vol. 165, no. 5/6, pp. 473–479.
22. Pickett, W.E., Electronic Structure of the High-Temperature Oxide Superconductors, *Rev. Mod. Phys.*, 1989, vol. 61, no. 2, pp. 433–512.
23. Tikhonova, I.R., Phase Equilibria, Structure, and Nons-toichiometry of Mixed Oxides in the Systems La–Me–Cu–O (M = Mn, Co), *Extended Abstract of Cand. Sci. (Chem.) Dissertation*, Yekaterinburg, 1999, p. 9.
24. Tikhonova, I.L., Zuev, A.Yu., and Petrov, A.N., Phase Equilibria and Crystal Structure of Phases in the System La(Sr)–Mn–Cu–O, *Zh. Fiz. Khim.*, 1998, vol. 72, no. 10, pp. 1794–1797.
25. Tovstolytkin, A.I., Pogorilyi, A.N., Belous, A.G., and Yanchevski, O.Z., Unusual Substitutional Properties of Cu in Bulk Polycrystalline Samples of $\text{La}_{0.7}\text{Ca}_{0.3}\text{Mn}_{1-x}\text{Cu}_x\text{O}_{3-\delta}$, *Low Temp. Phys.*, 2001, vol. 27, no. 5, pp. 366–371.
26. Borovskikh, L.V., Mazo, G.A., and Ivanov, V.M., Determination of the Average Oxidation State of Manganese in Mixed Manganites, *Vestn. Mosk. Univ., Ser. 2: Khim.*, 1999, vol. 40, no. 6, pp. 373–374.
27. Ullmann, H. and Trofimenko, N., Estimation of Effective Ionic Radii in Highly Defective Perovskite-Type Oxides from Experimental Data, *J. Alloys Compd.*, 2001, vol. 316, pp. 153–158.
28. Shannon, R.D., Revised Effective Ionic Radii and Systematic Studies of Interatomic Distances in Halides and Chalcogenides, *Acta Crystallogr., Sect. A: Cryst. Phys., Diff., Theor. Gen. Crystallogr.*, 1976, vol. 32, no. 5, pp. 751–767.
29. Abou-Ras, D., Boujelben, W., Cheikh-Rouhou, A., *et al.*, Effect of Strontium Deficiency on the Transport and Magnetic Properties of $\text{Pr}_{0.7}\text{Sr}_{0.3}\text{MnO}_3$, *J. Magn. Magn. Mater.*, 2001, vol. 233, pp. 147–154.
30. Dagotto, E., Motta, T., and Moreo, A., Colossal Magnetoresistant Materials: The Key Role of Phase Separation, *Phys. Rep.*, 2001, vol. 344, pp. 1–153.
31. Hiroyuki Kamata, Yuki Yonemura, Yurichiro Mizusaki, *et al.*, High Temperature Electrical Properties of the Perovskite-Type Oxide $\text{La}_{1-x}\text{Sr}_x\text{MnO}_3$, *J. Phys. Chem. Solids*, 1995, vol. 56, no. 7, pp. 943–950.
32. Nadgorny, B., Mazin, I.I., Osofsky, M., *et al.*, Origin of High Transport Spin Polarization in $\text{La}_{0.7}\text{Sr}_{0.3}\text{MnO}_3$: Direct Evidence for Minority Spin States, *Phys. Rev. B: Condens. Matter*, 2001, vol. 63, pp. 184433–184437.
33. Coey, J.M.D. and Sanvito, S., Magnetic Semiconductors and Half-Metals, *J. Phys. D: Appl. Phys.*, 2004, vol. 37, pp. 988–993.
34. Urushibara, A., Moritomo, Y., Arima, T., *et al.*, Insulator–Metal Transition and Giant Magnetoresistance in $\text{La}_{1-x}\text{Sr}_x\text{MnO}_3$, *Phys. Rev. B: Condens. Matter*, 1995, vol. 51, no. 20, pp. 14103–14109.
35. Akimoto, T., Maruyama, Y., Moritomo, Y., and Nakamura, A., Antiferromagnetic Metallic State in Doped Manganites, *Phys. Rev. B: Condens. Matter*, 1998, vol. 57, no. 10, pp. 5594–5597.
36. Budak, S., Ozdemir, M., and Aktas, B., Temperature Dependence of Magnetic Properties of $\text{La}_{0.67}\text{Sr}_{0.33}\text{MnO}_3$ Compound by Ferromagnetic Resonance Technique, *Physica B (Amsterdam)*, 2003, vol. 339, pp. 45–50.
37. Rivadulla, F., Hueso, L.E., Jardon, C., *et al.*, Effect of Porosity on FMR Linewidth of $\text{Ln}_{0.67}\text{A}_{0.33}\text{MnO}_3$ (Ln = La, Pr; A = Ca, Sr), *J. Magn. Magn. Mater.*, 1999, vols. 196–197, pp. 470–472.